

## A Multiscale Model of the Electrohysterogram The BioModUE\_PTL Project\*

Catherine Marque, Jérémy Laforêt, Chiara Rabotti, Asgeir Alexandersson, Guy Germain, Jean Gondry, Brynjar Karlsson, Brane Leskosek, Massimo Mischi, Charles Muszynski, Guid Oei, Jan Peuscher, and Drago Rudel

**Abstract**— The electrohysterogram (EHG) is a promising means of monitoring pregnancy and of detecting a risk of preterm labor. To improve our understanding of the EHG as well as its relationship with the physiologic phenomena involved in uterine contractility, we plan to model these phenomena in terms of generation and propagation of uterine electrical activity. This activity can be realistically modeled by representing the principal ionic dynamics at the cell level, the propagation of electrical activity at the tissue level and then the way it is reflected on the skin surface through the intervening tissue. We present in this paper the different steps leading to the development and validation of a biophysics based multiscale model of the EHG, going from the cell to the electrical signal measured on the abdomen.

### I. INTRODUCTION

The sequence of contraction and relaxation of the myometrium results from the electrical activity, deriving from the generation and propagation of cellular action potential bursts that induce mechanical contraction. The uterine electrical activity can be measured noninvasively on the woman's abdomen by surface electrodes. It is then referred to as the electrohysterogram (EHG) [1]. At the myometrial level, the cellular action potential generation has been previously modeled as a function of a large number of electrophysiological parameters related to ionic dynamics [2]. This model is physiology-based and has been shown to be representative of the main ionic mechanisms responsible for the genesis and evolution of the uterine electrical activity [2]. In order to understand the links existing between the physiological phenomena determining the efficiency of uterine contraction and the EHG signal characteristics, we

\*This work was funded by ANR, partner of the ERASysBio+ initiative supported under the EU ERA-NET Plus scheme in FP7.

C. Marque and J. Laforêt are with the Université de Technologie de Compiègne, UMR CNRS 7338, BP20529, 60205 Compiègne, France (e-mail: [catherine.marque@utc.fr](mailto:catherine.marque@utc.fr), [Jeremy.laforet@utc.fr](mailto:Jeremy.laforet@utc.fr))

C. Rabotti and M. Mischi are with Technological University Eindhoven, Signal Processing Systems, 5600 MB Eindhoven, the Netherlands (e-mail: [C.Rabotti@tue.nl](mailto:C.Rabotti@tue.nl), [M.Mischi@tue.nl](mailto:M.Mischi@tue.nl))

A. Alexandersson and B. Karlsson are with the Reykjavik University, EHG group, 103 Reykjavík, Iceland (e-mail: [alexandersson@gmail.com](mailto:alexandersson@gmail.com), [brynjar@hr.is](mailto:brynjar@hr.is))

G. Germain is with the MIRCEN, 92265 Fontenay-aux-Roses, France (e-mail: [guygermain@sfr.fr](mailto:guygermain@sfr.fr))

J. Gondry and C. Muszynski are with the CGO, 80000 Amiens, France (e-mail: [Gondry.Jean@chu-amiens.fr](mailto:Gondry.Jean@chu-amiens.fr), [Muszynski.Charles@chu-amiens.fr](mailto:Muszynski.Charles@chu-amiens.fr))

B. Leskosek and D. Rudel are with University of Ljubljana, IBMI, 1000 Ljubljana, Slovenia (e-mail: [brane.leskosek@mf.uni-lj.si](mailto:brane.leskosek@mf.uni-lj.si), [drago.rudel@mf.uni-lj.si](mailto:drago.rudel@mf.uni-lj.si))

G. Oei is with Máxima Medical Centre, MB Veldhoven, the Netherlands (e-mail: [G.Oei@mmc.nl](mailto:G.Oei@mmc.nl))

J. Peuscher is with Tms International, 7503 Enschede, the Netherlands (e-mail: [jan.peuscher@tmsi.com](mailto:jan.peuscher@tmsi.com))

designed the ERASysBio+ BioModUE\_PTL European project to develop a multiscale model of the uterine electrical activity, going from the cellular level to the signal recorded on the pregnant woman's abdomen.

### II. TOWARD A MULTISCALE MODEL STRUCTURE

#### A. Cellular level

We base our model on a cellular model previously developed and described in [2]. This model uses ten variables. An analysis of its dynamics has permitted to reduce it to a six-variable model, Red6 [3]. The signals simulated with Red6 are very similar to those obtained with the complete model. However, as this reduced model is still too computationally demanding to be used for propagation modeling at the tissue scale, we operate a further reduction by replacing the expression of calcium current  $I_{Ca}$  used in the complete model [2], which is the most computational intensive, by the one proposed by Parthimos et al. [4]. We thus obtain a less complex three-variable reduced model (Red3) described by the following equations:

$$\begin{aligned}\frac{dV_m}{dt} &= \frac{1}{C_m} (I_{stim} - I_{Ca} - I_K - I_{KCa} - I_{leak}), \\ \frac{dn_K}{dt} &= \frac{h_{n_K} - n_K}{\tau_{n_K}}, \\ \frac{d[Ca^{2+}]}{dt} &= f_c (-\alpha I_{Ca} - K_{Ca}[Ca^{2+}]),\end{aligned}$$

where  $V_m$  is the transmembrane potential,  $n_K$  the potassium activation variable,  $K_{Ca}$  the Calcium extraction factor and  $[Ca^{2+}]$  the intracellular calcium concentration. The ionic currents are defined as follows:

- $I_{Ca}$ , voltage dependent calcium channel current:

$$J_{back} + G_{Ca}(V_m - E_{Ca}) \frac{1}{1 + \exp\left(\frac{V_{Ca} - V_m}{R_{Ca}}\right)}$$

- $I_K$ , voltage dependent potassium channel current:

$$G_K n_K (V_m - E_K)$$

- $I_{KCa}$ , calcium dependent potassium channel current:

$$G_{KCa} \frac{[Ca^{2+}]^2}{[Ca^{2+}]^2 + k_d^2} (V_m - E_K)$$

- $I_L$ , leakage current:

$$G_L (V_m - E_L)$$

with  $J_{back}$  the background current,  $E_i$  and  $G_i$  the respective Nernst potential and the conductance for each ion  $i$ ,  $R_{Ca}$  the maximum slope of the voltage operated calcium channel (VOCC) activation,  $k_d$  the half-point potassium concentration. For more information, see [5].

Table I presents the computation time (in s) for the Red6 and the Red3 models, on various 2D grid sizes (from 100 to 5000

cells), obtained on a desktop computer (MacBookPro : 8 cores Intel Core i7 2.2Ghz, 8GB RAM, OSX 10.6 64bits) for 10s of simulated signal and by using the hybrid Euler integration method. Further improvement of the computation time has been obtained by using parallel computing [6].

TABLE I. COMPUTATION TIMES OF THE MODELS (IN SECONDS)

Number of cells	100	1000	2500	5000
Red6	109,6	296,6	616,5	1184,8
Red3	68,3	152,3	299,4	547,3

### B. Tissue level

To represent a sample of tissue, we simulate a rectangular grid of cells. Each individual cell is described with the *Red3* model and is electrically coupled with its neighbors. For this preliminary study, we use rectangular grids, with an equal distance between cells in all directions. The electrical coupling between the cells is computed by using a gap junction model, as proposed by Koenigsberger et al. [7]. It adds a coupling term to the  $\sum I_x/C_m$  reaction term initially described by *Red3*:

$$\frac{dV_m}{dt} = \frac{\sum I_x}{C_m} - \nabla \cdot D \nabla (V_m)$$

where  $I_x$  represent the different currents,  $C_m$  is the membrane capacitance and  $D$  the diffusion tensor. This tissue model can be 1D (cable-like line of cells), 2D (flat surface), or 2.5D (flat surface with non-null thickness).

### C. Organ level

In order to achieve a first approximation of the uterine anatomy, we first define a cylinder like 3D structure. This structure is far from being representative of the human uterus but is very close to the rat uterine structure. We will use it in order to generate signals at the organ level, by using, in that first case, model parameter values suitable for rat uterine cell modeling.

### D. Abdominal level

To model the propagation of signals towards the skin surface, we adapt the model proposed in [8]. It models the surface EHG, in the spatial frequency domain, as the product of an electrical source, the myometrial activity coming from the tissue level, and of an analytical expression representing the transfer function of the volume conductor. For this transfer function definition, the volume conductor is considered as made of parallel interfaces separating the 4 different abdominal tissues, namely: the myometrium, where the source is located at a depth  $y=y_0$ , the abdominal muscle, fat, and skin. The mathematical description of the volume conductor is derived by solving the Poisson equation at each interface. This description shows that the volume conductor effect depends on the tissue thicknesses, their conductivities, and the source depth,  $y_0$ . All the tissues are assumed to be isotropic with the exception of the abdominal muscle. (see [9] for more details). The original volume conductor model was developed for striated muscle, whose model is mainly 1D. We then adapt it for 2D modeling (tissue level source). We also add to the model the filtering effect of the recording electrodes and the presence of measurement noise [10].

The full multiscale model, from the cell to the abdominal levels, contains 26 parameters described in Annex.

## III. MODEL USE AND VALIDATION

### A. Data management system

In order to share information, documents, tools, models, guidelines and data, as well as to enable community networking, we built an integrating architecture facilitating single access points for the project partners. This architecture offers a Web portal framework, which integrates an interactive collaborative environment for information users and providers. The most important tool offered by this architecture is the database management system (EHG and tocographic signals -representing the mechanical effect of uterine contractions- and other metadata about patients). It offers indexing, search and data processing capabilities.

### B. Comparison to real signals

For model validation purpose, we use different approaches for each level. At the cellular level, the original model developed in [2] has been previously validated in comparison to bibliographic data. We thus compare our *Red3* model with the original complete model, in order to validate that the reduction process does not degrade significantly the *Red3* modeled signal characteristics.

For the tissue and organ level validation we plan to compare the signals with electrical uterine activity recorded either on pregnant cynomolgus monkeys by a telemetric system (recording protocol described in [11]), or on ex vivo rat uteri (recording protocol described in [12]).

For the abdominal level, we have defined a standardized human EHG recording protocol used by all the project partners [13]. The recorded EHG's will be used for comparison with simulated signals in different physiological/pathological situations.

All signals (from monkey, rat and woman) are stored in their respective databases.

### C. Sensitivity analysis

To study the sensitivity of the 26 model parameters, we use the principle of elementary effects as described by Morris [14]. This screening method is based on a "one factor at a time" design. It uses local variations (elementary effects) but averages them over several points in the parameter space. We assume no prior knowledge of the possible parameter variations and use uniform distributions bounded by  $\pm 20\%$  of their nominal value. For this sensitivity analysis, we do not use the simulated EHG signal itself, but features extracted from the signal. As a first step, we use 5 classical features: Root Mean Square amplitude (RMS), Time Reversibility (Trev), Power Spectral Density peak frequency (PF), linear ( $r_2$ ) and non-linear ( $h_2$ ) correlation coefficients.

## IV. RESULTS

### A. Cellular level

Figure 1 presents the comparison between the complete reference model [2] and *Red3*. We can notice that the difference between the two models is small (mean RMS

error about 11%), and that *Red3* can simulate different kinds of physiological activities (pregnancy and labor). We will then use *Red3* as the source of the electrical activity for the propagation to tissue, organ and abdominal levels.

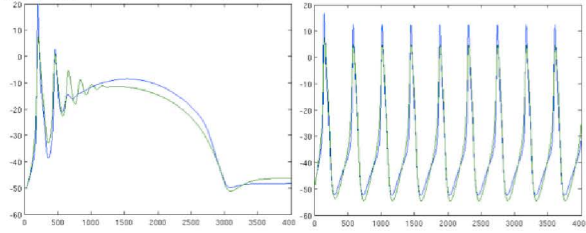


Figure 1. Comparison of the reference (Blue) [2] and the *Red3* models (green) for simulation of a pregnancy activity (left) and a labor burst (right).

### B. Tissue level

Figure 2 presents a snapshot taken at 1.16s of the propagation of one action potential simulated in a 2.5D structure (154 x 154 x 19 cells) corresponding to a 77 x 77 x 9.5 mm tissue piece with  $Dx=Dy=100*Dz$ . The electrical potential propagation starts at  $t=0s$  from the upper corner and its amplitude is color-coded.

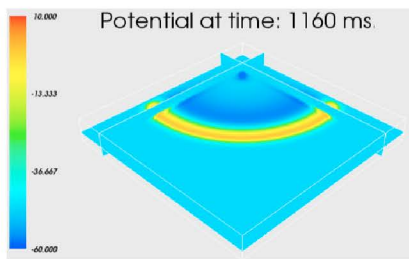


Figure 2. Representation of an action potential propagation across a 154 x 154 x 19 cells 2.5D piece of tissue. The potential amplitude is color-coded.

### C. Organ level

Figure 3 presents a snapshot taken at 3.4 s of the propagation of a burst of action potentials simulated in a 2D cylindrical structure (500 x 500 x 1 cells). The electrical potential propagation starts from the upper right extremity  $t=0s$  and the amplitude is color-coded.

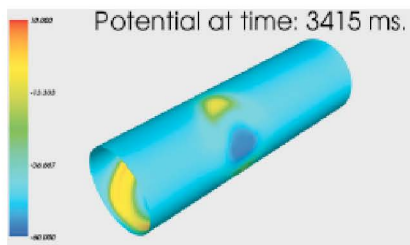


Figure 3. Representation of action potential propagation across a 500 x 500 x 1 cells piece of tissue. The potential amplitude is color-coded.

### D. Abdominal level

We first implemented the abdominal model by using a 1D representation (one line of cells generating the electrical activity). Figure 4 presents the results obtained by using this 1D representation. The simulated signal (left) is compared to a real signal (right) recorded on a delivering parturient. We can observe some clear similarities between the two signal

components (red rectangles), the real EHG being more complex and/or noisy. After this first feasibility test, we implemented the volume conductor in 2D, with the organ level 2.5D source, in order to get closer to real recording situations and to real signals.

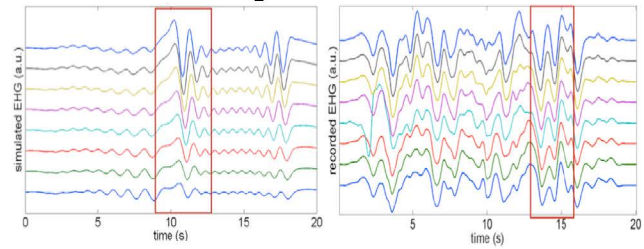


Figure 4. Representation of a simulated EHG computed with a 1D configuration (left) and a real EHG (right) recorded during labor.

Figure 5 presents one example of the EHG's obtained with a 2D volume conductor and the same electrode grid as the one developed for human recording in our standardization process [12], used by all the project partners for EHG recordings. We will further use this volume conductor and this electrode configuration for the whole model validation and parameter identification.

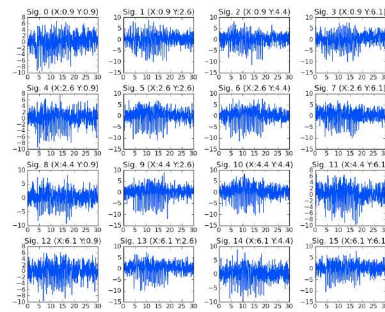


Figure 5. Simulated monopolar EHG signals with a 2D volume conductor.

### E. Sensitivity analysis

The first results of the sensitivity analysis indicate that only 4 features among the 5 studied are sensitive to parameter model variations: RMS,  $T_{rev}$ ,  $r_2$  and  $h_2$ . The results presented in Table II are sorted by rank for each feature, the lower rank "1" being given to the higher influence of a parameter on the given feature. Table II presents only the ranking results for the model parameters that have significant influences on these 4 features (greater than 1/1000 of the maximal value). The values indicated in the columns represent the rank of a parameter for each given feature. The lower the value, the higher the parameter influence on the given feature. A number of relevant observations can be derived from these results:

- 18 over the 26 model parameters present a significant influence on at least 3 features
- some parameters have very different influences on the different features (e.g.  $snr$ ,  $EI$ )
- some parameters have a strong influence on every features (e.g.  $ERay$ ,  $vca2$ )

This analysis will be the first step towards the parameter identification process that will use real signals to identify the



values of difficult to measure physiological parameters, for each modeling level.

## V. CONCLUSION

We developed in this project the first simplified multiscale model of the uterine electrical activity recorded on the abdominal wall, the EHG. This model includes all the steps going from the cellular ionic channel dynamics to the abdominal wall and recording electrode characteristics. It enables the simulation of EHG's based on the main physiological phenomena involved in uterine contractility, such as cell excitability and uterine synchronization. The next step for the model structure will be to approach a 3D representation of a human uterus. Then, we will go further in the model analysis and validation, in order to identify, by comparing simulated EHG's to real ones, the physiological /pathological ranges of the model parameters. This will require a dedicated identification process based on the sensitivity analysis. The developed Web portal with EHG database management system will support the model design, enabling validation of the model. When validated, this EHG model will be used with a model-aided diagnosis approach for the detection of preterm labor, based on EHG analysis.

TABLE II. SENSITIVITY ANALYSIS

Parameters	RMS	Trev	r2	h2
a	18	16	9	14
alpha	11	13	5	10
Ek	6	2	11	5
El	12	8	*	11
ERay	1	1	2	1
fc	16	14	4	6
Gca2	8	6	14	15
Gk	15	11	13	17
Gkca	9	12	7	13
Gl	5	9	15	4
Iback	17	15	*	16
Kca	10	17	8	8
Kd	14	7	12	18
Rca	3	4	10	7
Sigma_m	4	3	6	9
snr	7	*	1	2
T	14	10	16	12
vca2	2	5	3	3

\*represents a non significant influence of the parameter on the given feature

## REFERENCES

[1] D. Devedeux, C. Marque, S. Mansour, G. Germain, and J. Duchêne "Uterine electromyography: a critical review". *Am. J. Obstet. Gynecol.*, vol. 169, pp.1636–1653, 1993.

[2] S. Rihana, J. Terrien, G. Germain, and C. Marque "Mathematical modeling of electrical activity of uterine muscle cells". *Medical and Biological Engineering and Computing*, vol. 47, pp.665–675, 2009.

[3] S. Rihana, J. Santos, S. Mondie, and C. Marque "Dynamical analysis of uterine cell electrical activity model". *Conf. Proc. IEEE Eng. Med. Biol. Soc.*, vol. 1, pp. 4179–4182, 2006.

[4] D. Parthimos, D. H. Edwards, and T. M. Griffith "Minimal model of arterial chaos generated by coupled intracellular and membrane Ca<sup>2+</sup> oscillators". *Am. J. Physiol.*, vol. 277, no. 3 Pt 2, pp. H1119–H1144, Sep 1999.

[5] J. Laforet, C. Rabotti, J. Terrien, M. Mischi and C. Marque "Toward a

multiscale model of the uterine electrical activity". *IEEE Transactions on Bio-Medical Engineering*, 58:3487–3490, 2011.

[6] T. Hedrich, J. Laforet and C. Marque "Simulations of uterine electrical activity using parallel computing". *International Workshop on Innovative Simulation for Healthcare*, Vienna, Austria, September 2012

[7] M. Koenigsberger, R. Sauser, M. Lambole, J.-L. Bny, and J.-J. Meister "Ca<sup>2+</sup> dynamics in a population of smooth muscle cells: modeling the recruitment and synchronization". *Biophys. J.*, vol. 87, no. 1, pp. 92–104, Jul 2004.

[8] C. Rabotti, M. Mischi, L. Beulen, S.G. Oei, and J.W.M. Bergmans "Modeling and identification of the electrohysterographic volume conductor by high-density electrodes". *IEEE Trans. Biomed. Eng.*, 57:519–527, 2010.

[9] J. Laforet, C. Rabotti, J. Terrien, M. Mischi, and C. Marque, "Improved multi-scale modeling of uterine electrical Activity," IRBM, to be published.

[10] J. Laforet and C. Marque, "uEMG: Uterine EMG simulator". *VIIth International Workshop on Biosignal Interpretation, BSI2012*, Como, Italy, July 2012.

[11] J. Terrien, M. Hassan, G. Germain, C. Marque and B. Karlsson "Nonlinearity testing in the case of non Gaussian surrogates, applied to improving analysis of synchronicity in uterine contraction". *Proc. IEEE 31th Eng. Med. Biol. Soc. Minneapolis*, Minnesota, USA, pp. 3477-3480, 2009.

[12] A. Chkeir, M. Hassan, B. Karlsson, M-J Fleury and C. Marque, "Patterns of synchronization of electrical activity in the pregnant rats uterus". *Medical & Biological Engineering & Computing*, submitted for publication.

[13] M. Hassan, J. Terrien, B. Karlsson and C. Marque, "Comparison between approximate entropy, correntropy and time reversibility: Application to uterine EMG signals". *Medical Engineering & Physics*. 33 (8), 980-986, 2011.

[14] M. Morris, "Factorial sampling plans for preliminary computational experiments," *Technometrics*, vol. 33, no. 2, pp. 161–174, 1991.

## ANNEX: MODEL PARAMETERS

Model	Name	Description
Cell	alpha	Current conservation factor
	EL	Leak Nernst potential
	EK	Potassium Nernst potential
	fc	Calcium influx probability
	GCa	VOCC conductance
	Gk	Potassium channels conductance
	GkCa	K/Ca channels conductance
	GL	Leak channels conductance
	Iback	Background calcium current
	kCa	Ca extraction factor
	kd	Half-point potassium concentration
	RCa	Maximal slope of the VOCC activity
	T	Temperature
	VCa2	Half-point of the VOCC activity
Tissue/Organ	Dx	Diffusion coefficient (x axis)
	Dy	Diffusion coefficient (y axis)
Volume conductor	a	Abdominal muscle thickness
	s	Skin thickness
	f	Fat tissue thickness
	Sigma_ax	Abdominal muscle conductivity (x axis)
	Sigma_ay	Abdominal muscle conductivity (y axis)
	Sigma_f	Fat tissue conductivity
	Sigma_m	Myometrium conductivity
	Sigma_s	Skin conductivity
Recording	Eray	Electrode radius
	snr	EHG signal to noise ratio